Exergetic, economic and environmental (3E) analyses, and multi-objective optimization of a CO_2/NH_3 cascade refrigeration system

Mehdi Aminyavari [a], Behzad Najafi [b], Ali Shirazi [c,*], Fabio Rinaldi [b]

[a] Scuola di Ingegneria Industriale, Campus di Piacenza, Politecnico di Milano, Via Scalabrini, 76, 29100 Piacenza, Italy
[b] Dipartimento di Energia, Politecnico di Milano, Via Lambruschini 4, 20156 Milano, Italy
[c] School of Mechanical and Manufacturing Engineering, The University of New South Wales (UNSW), Kensington, New South Wales 2052, Australia

Received 3 July 2013
Accepted 29 December 2013
Available online 6 January 2014

1. Introduction

In consequence of environmental issues related to the global warming and ozone layer depletion attributed to the application of synthetic refrigerants (CFC's, HCFC's and HFC's), the return to the utilization of natural materials for refrigeration purposes appears to be an appropriate alternative. Accordingly, the natural refrigerants such as ammonia, carbon dioxide and hydrocarbons, have recently received increasing attentions [1].

In refrigeration systems involving a high temperature difference between the heat source and the heat sink, employing a single stage refrigeration system is not economical owing to the fact that the corresponding high pressure ratio leads to a low volumetric efficiency of the compressors and consequently low coefficient of performance of the system. In addition, utilizing a refrigerant in a wide temperature range results in a decrement in evaporator pressure and an increment in suction volume and condenser pressure [2]. Employing cascade refrigeration systems is an appropriate solution to evade aforementioned issues. CO_2/NH_3 cascade system is a well-known system in refrigeration industry in which two natural refrigerants are used. Ammonia, despite its apparent disadvantages of toxicity and moderate flammability [3], is a natural refrigerant which has been most commonly adopted in the high temperature cycle of two-stage refrigeration systems. Owing to the fact that at low temperatures (under $-35\ ^\circ C$), it has a

* Corresponding author. Tel.: +61 413077896.
E-mail addresses: mehdi.aminyavari@mail.polimi.it (M. Aminyavari), behzad.najafi@mail.polimi.it (B. Najafi), a.shirazi@student.unsw.edu.au (A. Shirazi), fabio.rinaldi@polimi.it (F. Rinaldi).

Nomenclature

A	area (m^2)
$\dot{C}$	cost rate (US$ s^{-1})
C_{CO_2}	unit damage cost of carbon dioxide emissions (US$ Kg^{-1} CO_2)
C_{elec}	electricity unit cost (US$ $(kW\ h)^{-1}$)
C_p	specific heat at constant pressure (kJ kg^{-1} K^{-1})
CFC	chlorofluorocarbon
CRF	capital recovery factor
E	energy (kJ)
$\dot{E}$	exergy flow rate (kW)
$\overline{e}$	specific exergy (kJ $kmol^{-1}$)
h	specific enthalpy (kJ kg^{-1})
i	interest rate
HCFC	hydrochlorofluorocarbon
HFC	hydrofluorocarbon
HTC	high temperature circuit
k	specific heat ratio
LTC	low temperature circuit
$\dot{m}$	mass flow rate (kg s^{-1})
N	operational hours in a year
n	system lifetime (year)
$\dot{n}$	molar flow rate (kmol s^{-1})
p	pressure (kPa)
$\dot{Q}$	the time rate of heat transfer (kW)
r_P	pressure ratio
$\overline{R}$	universal gas constant (kJ $kmol^{-1}$ K^{-1})
s	specific entropy (kJ kg^{-1} K^{-1})
T	temperature (K or °C)
TOPSIS	Technique for Order Preference by Similarity to an Ideal Solution
$\dot{W}$	mechanical work (kW)
X	molar fraction
Z	capital cost (US$)
$\dot{Z}$	capital cost rate (US$ s^{-1})

Greek symbols

η	efficiency
μ	emission conversion factor of electricity from grid (kg $(kW\ h)^{-1}$)
Φ	maintenance factor
Δ	difference

Subscripts

0	ambient, reference
C	condenser
CAS	cascade condenser
CL	cold space
comp	compressor
cond	condenser
CV	control volume
D	destruction
e	exit
elec	electrical
env	environmental
evap	evaporator
exp	expansion valve
H	high temperature
i	inlet
L	low temperature
m	mechanical
MC	cascade condenser (middle)
ME	cascade evaporator (middle)
op	operation
p	pressure
s	isentropic

Superscript

CH	chemical
PH	physical
Q	heat transfer
W	work

vapor pressure lower than atmospheric pressure, which may cause air leakage into the system, ammonia cannot be used in the low temperature circuit. In contrast, carbon dioxide is a non-toxic, non-flammable gas with a positive vapor pressure at temperatures below −35 °C which makes it a suitable choice for low temperature cascade cycle [3]. Therefore, ammonia and carbon dioxide have been shown to be the most promising natural refrigerants across a broad spectrum of commercial and industrial refrigeration and air-conditioning systems [4].

Experimental studies have been carried out on performance of CO_2/NH_3 cascade systems and the effect of operating parameters such as the evaporation and condensation temperatures of the low temperature circuit (LTC) on the performance of the system were investigated [1,5]. Some studies have been conducted on the theoretical analysis of cascade refrigeration system based on the first law of thermodynamic [1,6]. A similar study was also carried out by Messineo [7] in which a comparison between the CO_2/NH_3 cascade refrigeration system and a hydrofluorocarbon (HFC) two-stage system was performed. Lee et al. [3] presented an energetic-exegetic analysis of CO_2/NH_3 cascade system in order to maximize the COP and minimize the exergy destruction of the system.

Economic considerations should also be taken into account while analyzing a refrigeration plant. Thermo-economic method is a proper approach for analyzing the systems from both thermodynamic and economic points of view [8]. Mitishita et al. [9] performed a thermo-economic design and optimization of frost-free refrigerators. Rezayan and Behbahaninia [2] carried out a similar study on CO_2/NH_3 system.

Multi-objective optimization method is an efficient approach for optimizing the problems dealing with conflicting objectives, the approach which has been successfully utilized for optimization of heat exchangers [10–14]. Gebreslassie et al. [15] performed multi-objective optimization on sustainable single-effect water/lithium bromide absorption cycle. Sanaye and Shirazi [16] applied the multi objective optimization on an ice thermal energy storage (ITES) system .Navidbakhsh and Shirazi [17] also applied a similar optimization method on a PCM incorporated ITES system for air conditioning applications.

In the present paper, thermodynamic (energetic and exergetic), economic, and environmental analyses as well as multi-objective optimization of a CO_2/NH_3 cascade refrigeration system are carried out. The refrigeration system is modeled and validated based on the results of a previous study. Afterward, considering the exergetic efficiency (to be maximized) and the total cost rate of the system (to be minimized) as objective functions, multi-objective optimization of the system is performed. The capital and maintenance costs of system components, the operational cost, and the social cost due to CO_2 emission are included in the total cost rate of the plant. Applying the mentioned optimization approach, a set of

optimal solutions, called Pareto front, is achieved. In the next step, Euclidean method is employed for non-dimensionalization of the Pareto front results and the TOPSIS method is utilized to choose a final optimum design point. A sensitivity analysis has been performed in order to study the effect of variation of unit cost of electricity on the Pareto front. The effect of the variation of the cooling load on the exergy destruction within the systems is also investigated.

2. Mathematical modeling

2.1. Description of cascade refrigeration cycle

A schematic layout of the CO_2/NH_3 refrigeration cycle which has been considered in the present study is demonstrated in Fig. 1. The system consists of two separate circuits including a high temperature circuit (HTC) and a low temperature one (LTC). Ammonia is used as the refrigerant in the high temperature circuit while in the low temperature circuit carbon dioxide is employed as the refrigerant. Each refrigeration system consists of a compressor, a condenser, an expansion valve, and an evaporator. The two circuits are thermally coupled to each other through a cascade condenser, which acts as an evaporator for the HTC and a condenser for the LTC.

The evaporator of LTC absorbs the cooling load $\dot{Q}_L$ from the cooling space in the evaporating temperature T_E. The condenser in HTC rejects heat flow of $\dot{Q}_H$ at condensing temperature of T_C to the ambient which has the temperature of T_0. The heat transferred from the condenser of LTC to the evaporator of HTC in the cascade condenser is equal to the sum of the absorbed heat by the evaporator of the LTC and the work input to the LTC compressor. Similarly, the heat rejected from the HTC condenser is equal to the sum of the heat absorbed by the evaporator of HTC and the work input to the HTC compressor. The cascade condenser temperature difference, ΔT_{CAS} is the difference between the evaporation temperature of ammonia and the condensation temperature of carbon dioxide, which are called T_{ME} and T_{MC} respectively. The T–S diagram of the cycle is also illustrated in Fig. 2.

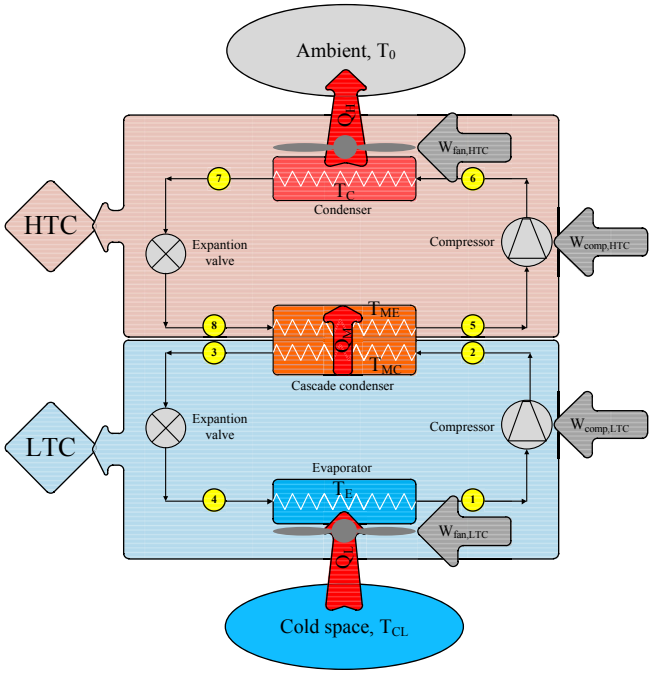

Fig. 1. Schematic diagram of the CO_2/NH_3 refrigeration cycle.

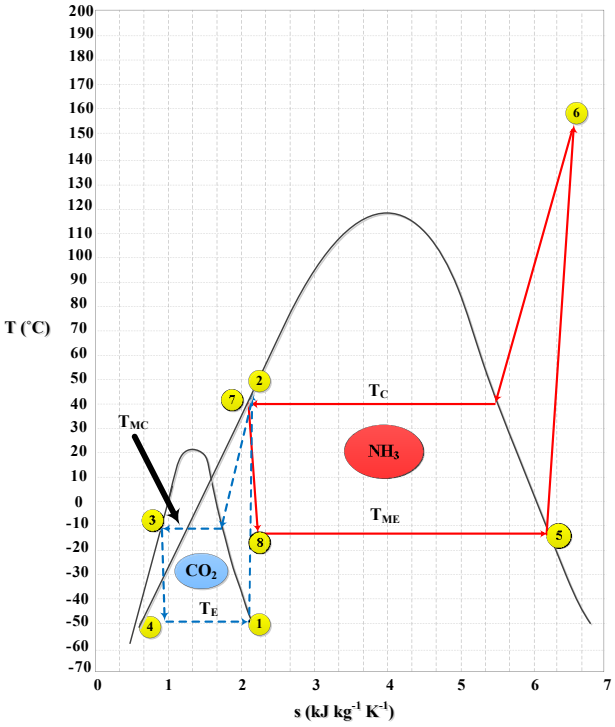

Fig. 2. T-S diagram of the CO_2/NH_3 refrigeration cycle.

2.2. Energetic analysis

The thermodynamic analysis of the cascade refrigeration system was performed based on the following general assumptions:

- Pressure and heat losses/gains in the pipe networks or system components are negligible.
- The changes in kinetic and potential energy are negligible.
- All system components operate under steady-state conditions.
- Gas leakage is negligible in all the joints connecting the pipes to each component.

The thermodynamic properties of CO_2 and NH_3 were determined using REFPROP [18]. It should also be pointed out that since the model is developed in MATLAB® environment, a specific MATLAB® function is employed which calls the REFPROP data base to obtain the thermodynamic data. The governing equations based on the energy balances for system components are obtained as follows:

The cooling load of the system absorbed by the LTC evaporator from the cold space should be equal to the enthalpy difference of CO_2 across the evaporator multiplied by its mass flow rate:

$$\dot{Q}_L = \dot{m}_L(h_1 - h_4) \tag{1}$$

The isentropic efficiency of the LTC compressor (η_s) is considered as follows [1]:

$$\eta_S = 1 - (0.04 \times r_P) \tag{2}$$

The mechanical and electrical efficiencies of the compressor (η_m and η_e) are considered to be 0.93 [2].

Applying the energy balance on the system, the compressor power consumption ($\dot{W}_{LTC,comp}$) is obtained as:

$$\dot{W}_{LTC,comp} = \frac{\dot{m}_L(h_{2S} - h_1)}{\eta_s\eta_m\eta_e} = \frac{\dot{m}_L(h_2 - h_1)}{\eta_m\eta_e} \tag{3}$$

Following the same approach used for the LTC compressor, $\dot{W}_{HTC,comp}$ can be calculated as follows:

$$\dot{W}_{HTC,comp} = \frac{\dot{m}_H(h_{6S} - h_5)}{\eta_s \eta_m \eta_e} = \frac{\dot{m}_H(h_6 - h_5)}{\eta_m \eta_e} \quad (4)$$

$\eta_m \eta_e$ for the HTC compressor are similarly considered to be 0.93 and the isentropic efficiency η_s is also similarly calculated using Eq. (2)

As it has been previously mentioned, both of the expansion valves in LTC and HTC are assumed to be isenthalpic, so:

$$h_3 = h_4 \quad (5)$$

and

$$h_7 = h_8 \quad (6)$$

The heat rate exchanged from LTC to HTC in the cascade condenser is called $\dot{Q}_M$ and can be calculated as:

$$\dot{Q}_M = \dot{m}_H(h_5 - h_8) = \dot{m}_L(h_2 - h_3) \quad (7)$$

The energy balance equation for HTC condenser can be expressed by:

$$\dot{Q}_H = \dot{m}_H(h_6 - h_7) \quad (8)$$

Writing the first law of thermodynamics for the whole system as a control volume results in:

$$\dot{Q}_H = \dot{Q}_L + \dot{W}_{LTC,comp} + \dot{W}_{HTC,comp} \quad (9)$$

2.3. Exergetic analysis

Exergy is defined as the maximum obtainable work that a system can yield in a given state when it comes to the environment conditions. The method of exergetic analysis is based on the second law of thermodynamics and enables the designers to identify location, cause and true magnitude of wastes and losses in thermal systems [19].

Applying the first and second laws of thermodynamics, the steady state form of exergy balance equation for a control volume can be expressed as follows:

$$\frac{dE_{CV}}{dt} = \sum_j \dot{E}_j^Q - \dot{E}^W + \sum_i \dot{E}_i - \sum_e \dot{E}_e - \dot{E}_D = 0 \quad (10)$$

Where $\dot{E}_i$ and $\dot{E}_e$ are the exergy transfer rate at control volume inlets and outlets, $\dot{E}_D$ is the exergy destruction rate due to irreversibilities, $\dot{E}^W$ is the rate of exergy transfer by work, and $\dot{E}^Q$ is the rate of exergy transfer by heat transfer, respectively.

In absence of electromagnetic, electric, nuclear, and surface tension effects and assuming negligible values of change in potential and kinetic energy, the exergy flow rate of the system is divided into two parts of physical and chemical exergy [19,20]:

$$\dot{E} = \dot{E}^{PH} + \dot{E}^{CH} \quad (11)$$

The physical exergy can be determined by:

$$\dot{E}^{PH} = \dot{m}[(h - h_0) - T_0(s - s_0)] \quad (12)$$

Writing the exergy balance equation (Eq. (10)) for each system component, the exergy destruction rate of each component is obtained as:

$$\dot{E}_{D,evap+fan} = \left(1 - \frac{T_0}{T_{CL}}\right)\dot{Q}_L + \left(\dot{E}_4 - \dot{E}_1\right) + \dot{W}_{fan,evap} \quad (13)$$

$$\dot{E}_{D,LTC,comp} = \left(\dot{E}_1 - \dot{E}_2\right) + \dot{W}_{LTC,comp} \quad (14)$$

$$\dot{E}_{D,LTC,exp} = \left(\dot{E}_3 - \dot{E}_4\right) \quad (15)$$

$$\dot{E}_{D,cas} = \left(\dot{E}_2 + \dot{E}_8\right) - \left(\dot{E}_3 + \dot{E}_5\right) \quad (16)$$

$$\dot{E}_{D,HTC,comp} = \left(\dot{E}_5 - \dot{E}_6\right) + \dot{W}_{HTC,comp} \quad (17)$$

$$\dot{E}_{D,HTC,exp} = \left(\dot{E}_7 - \dot{E}_8\right) \quad (18)$$

$$\dot{E}_{D,cond+fan} = \left(\frac{T_0}{T_0} - 1\right)\dot{Q}_H + \left(\dot{E}_6 - \dot{E}_7\right) + \dot{W}_{fan,cond} \quad (19)$$

It should be noted that the power consumption of fan of the evaporator and that of the condenser, as a parasitic load, has been added to the exergy destruction of these components.

The total inlet exergy into the system can be found as:

$$\dot{E}_{in} = \dot{W}_{HTC,comp} + \dot{W}_{LTC,comp} + \dot{W}_{fan,cond} + \dot{W}_{fan,evap} \quad (20)$$

The outlet exergy of the system can also be determined as:

$$\dot{E}_{out} = \dot{Q}_L\left(\frac{T_0}{T_{CL}} - 1\right) \quad (21)$$

Hence, the total exergy destruction can be calculated as:

$$\dot{E}_{D,totall} = \dot{E}_{in} - \dot{E}_{out} = \sum_k \dot{E}_{D,k} \quad (22)$$

where $\sum_k \dot{E}_{D,k}$ stands for the sum of the exergy destructions of system components.

Finally, the exergetic efficiency of the system can be determined by:

$$\eta_{II} = \frac{\dot{E}_{out}}{\dot{E}_{in}} = 1 - \frac{\dot{E}_{D,totall}}{\dot{E}_{in}} \quad (23)$$

2.4. Economic analysis

In this paper, the capital and maintenance costs of components together with the operational cost of the plant have been taken into account. In order to consider the effect of emissions, the social cost of the CO_2 emissions have also been included. Accordingly, the total cost rate of the cascade system ($\dot{C}_{tot}$) including the capital and maintenance costs ($\sum_k \dot{Z}_k$), operational cost ($\dot{C}_{op}$), and the penalty cost due to CO_2 emission ($\dot{C}_{env}$) can be expressed as follows:

$$\dot{C}_{tot} = \sum_k \dot{Z}_k + \dot{C}_{op} + \dot{C}_{env} \tag{24}$$

2.4.1. Investment and maintenance costs

The capital cost of each component (Z_k) is estimated based on the cost functions which are listed below [2]:

$$Z_{HTC,comp} = 9624.2\dot{W}^{0.46}_{HTC,comp} \tag{25}$$

$$Z_{LTC,comp} = 10167.5\dot{W}^{0.46}_{LTC,comp} \tag{26}$$

$$Z_{cond} = 1397A^{0.89}_{o,cond} + 629.05\dot{W}^{0.76}_{fan,cond} \tag{27}$$

$$Z_{evap} = 1397A^{0.89}_{o,evap} + 629.05\dot{W}^{0.76}_{fan,evap} \tag{28}$$

$$Z_{cas.cond} = 2382.9A^{0.68}_{o,cas.cond} \tag{29}$$

In engineering economics, the unit of time interval considered for evaluation of the capital cost is usually taken as a year and the corresponding cost is obtained using the capital recovery factor (CRF), which can be determined by [20]:

$$CRF = \frac{i(1+i)^n}{(1+i)^n - 1} \tag{30}$$

where the terms i and n stand for the interest rate and the system lifetime, respectively.

Moreover, to convert the capital cost (in terms of US dollar) into the cost per unit of time $\dot{Z}_k$, one may write:

$$\dot{Z}_k = \frac{Z_k \times CRF \times \Phi}{N \times 3600} \tag{31}$$

where N and Φ are the annual operational hours of the system and the maintenance factor, respectively. Applying Eq. (31) for each system component, the investment and maintenance cost rate of the whole system ($\sum_k \dot{Z}_k$) is:

$$\sum_k \dot{Z}_k = \dot{Z}_{HTC,comp} + \dot{Z}_{LTC,comp} + \dot{Z}_{cond} + \dot{Z}_{evap} + \dot{Z}_{cas.cond} \tag{32}$$

2.4.2. Operational cost

The operational cost of this system is due to the cost associated with the power consumption of compressors and fans which can be expressed as follows:

$$\dot{C}_{op} = \left(\dot{W}_{Comp,LTC} + \dot{W}_{Comp,HTC} + \dot{W}_{Fan,LTC} + \dot{W}_{Fan,HTC}\right) \times \frac{C_{elec}}{3600} \tag{33}$$

where C_{elec} is the unit cost of electricity during the working hours of the system.

2.5. Environmental analysis

Due to the increasing environmental concerns and specifically global warming issues, considering the environmental impacts is becoming essential in modeling of the thermal systems. In this regard, the amount of CO_2 emission is considered as an important factor in the present work and as shown in Eq. (34) its respective social cost is added to the total cost rate of the cycle in the system optimization procedure [16].

$$m_{CO_2}[kg] = \mu_{CO_2}\left[\text{kg kWh}^{-1}\right] \times \text{annual electricity consumption[kWh]} \tag{34}$$

where μ_{CO_2} is the emission conversion factor of electricity from grid and its value is 0.968 kg (kW h)$^{-1}$ [21]. Thus, the rate of penalty cost for CO_2 emission ($\dot{C}_{env}$) is defined as follows:

$$\dot{C}_{env} = \frac{\left(\frac{m_{CO_2}}{1000}\right) \times C_{CO_2}}{N \times 3600} \tag{35}$$

where C_{CO_2} is the unit damage cost of carbon dioxide emission.

3. System optimization

3.1. Multi-objective optimization

Multi-objective optimization is a realistic approach for handling real-world problems dealing with conflicting objectives. The advantage of this procedure is the ability to optimize the system considering any number of conflicting objectives simultaneously while taking into account several equality and inequality constraints. Apparently, there is no single solution which can satisfy the conflicting objectives simultaneously and accordingly the optimum solution of a multi-objective optimization cannot be unique. Hence, a logical solution to a multi-objective problem is obtaining a set of non-dominated solutions; each of which satisfies the objectives at an acceptable level [13,22]. After determining the set of solutions, the 'Pareto optimal set', a decision-maker can decide which of the obtained design sets is suitable for the considered specific project [11,12]. In conclusion, a multi-objective optimization problem can be defined as:

$$\text{Find } \mathbf{x} = (\mathbf{x}_i) \quad \forall i = 1, 2, \ldots, N_{par}$$

$$\text{Minimizing or maximizing } f_i(\mathbf{x}) \quad \forall i = 1, 2, \ldots, N_{obj}$$

$$g_j(\mathbf{x}) = 0 \quad \forall j = 1, 2, \ldots, m$$

$$h_k(\mathbf{x}) \le 0 \quad \forall k = 1, 2, \ldots, n$$

Table 1
Considered design parameters for system optimization and their corresponding range of variation.

Design parameter	Range of variation
CO_2 evaporation temperature	$-56\,^{\circ}C < T_E < -47\,^{\circ}C$
CO_2 condensation temperature	$-11\,^{\circ}C < T_{MC} < 1\,^{\circ}C$
Cascade temperature difference	$2\,^{\circ}C < \Delta T_{CAS} < 10\,^{\circ}C$
NH_3 condensation temperature	$40\,^{\circ}C < T_C < 65\,^{\circ}C$

where $\mathbf{x}$, N_{par}, $f_i(\mathbf{x})$, N_{obj}, $g_j(\mathbf{x})$ and $h_k(\mathbf{x})$ are decision variables vectors, number of decision variables, objectives, number of objectives, equality and inequality constraints respectively [22].

In this paper, the considered objective functions are the exergetic efficiency (objective functions I, Eq. (23)) and total cost rate (objective function II, Eq. (24)) of the whole cascade system which should be maximized and minimized respectively. The list of the design parameters (decision variables) which has been chosen for optimization of the system has been listed in Table 1.

3.2. Genetic algorithm

The genetic algorithm (GA) method is a heuristic technique inspired by the Darwin's laws of natural selection [23]. In this algorithm, a solution vector (design parameters vector) is called a chromosome and is made of discrete units called genes which determine its features. GAs are promising techniques for solving the multi-objective optimization problems [23]. New generations of solutions are produced from the previous ones employing two operators; crossover and mutation. In the crossover operation, two chromosomes (parents) are combined together to form new chromosomes (offsprings). Considering the fact that individuals with higher fitness have more chance for being chosen and generating offsprings, the new population will attain better genes, the fact which results in convergence to an overall good solution. In the mutation operator, random changes into the properties of chromosomes are applied. Considering the fact that these changes are not significant and depend on the length of the chromosomes, the new chromosomes produced by mutation will not be very different from the original ones. Mutation operator helps the population search to escape from local optima by introducing diversity into the population [23]. The flowchart in Fig. 3 represents various stages of GAs optimization process.

As the search evolves, the population converges, and eventually is dominated by a set of solutions called the Pareto optimal set. After determining the Pareto optimal set, a decision-maker must decide which of the achieved design vectors is suitable for the specific project. In the present work, the multi-objective GA in MATLAB® optimization toolbox has been implemented to optimize the objective functions presented in Eqs. (23) and (24).

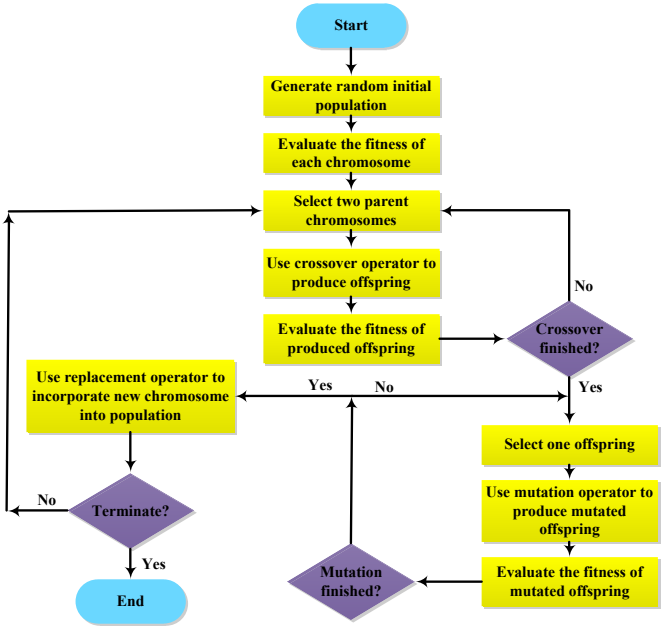

Fig. 3. Flowchart of genetic algorithm technique for system optimization.

Table 2
Input parameters used for simulation of cascade refrigeration system.

Parameter	Value
Cooling capacity ($\dot{Q}_L$)	50 kW
Ambient temperature (T_0)	25 °C
Ambient pressure (P_0)	1 atm
Cold refrigerated space temperature (T_{CL})	−45 °C

4. Case study

The mentioned modeling and optimization techniques are applied for optimal design of a cascade refrigeration system to be installed in Shahsavar, a city in north of Iran. The cooling capacity of the system is 50 kW. The main input parameters used for simulation of the system are listed in Table 2.

The unit cost of electricity (C_{elec}) is considered to be 0.06 US$ (kW h)$^{-1}$ [22]. Furthermore, the unit damage cost of carbon dioxide emission (C_{CO_2}) is considered to be 90 US dollars per ton of carbon dioxide emissions [24].

To determine the CRF (Eq. (30)), the approximate lifetime of the system (n), the maintenance factor (Φ), and the annual interest rate (i) are considered as 15 years, 1.06, and 14% [25] respectively. The annual operational hours of the cogeneration system (N) is considered to be 7000 h.

5. Results and discussion

5.1. Model verification

In order to validate the modeling results of the CO_2/NH_3 refrigeration system, the basic performance parameters of the system including the exergy destruction rate of all components as well as the total exergy destruction rate of the system ($\dot{E}_D$), the exergetic efficiency (η), and also the COP of the system obtained from the developed model have been compared with the corresponding results reported in Ref. [1].

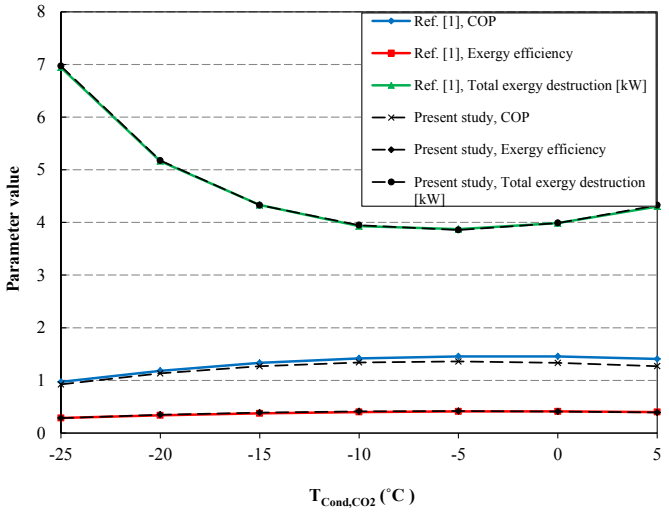

Fig. 4. Comparison between the COP, exergetic efficiency, and total exergy destruction, which are generated by the results of the present model and the data from a previous study [1].

Table 3
Comparison of computed values of exergy destruction rate of system components obtained from modeling of the system with the corresponding values reported in Ref. [1] (R: reported; M: modeling; D: difference (%)).

T_{Cond,CO_2}	$\dot{E}_{D,E,CO_2}$			$\dot{E}_{D,Comp,CO_2}$			$\dot{E}_{D,EX,CO_2}$			$\dot{E}_{D,CAS}$		
	R	M	D	R	M	D	R	M	D	R	M	D
25 °C	0.2637	0.2581	2.12	0.1383	0.1290	6.72	0.1469	0.1577	7.35	0.3446	0.3442	0.12
−20 °C	0.2637	0.2725	3.33	0.1967	0.2008	2.08	0.2135	0.2151	0.75	0.3856	0.3729	3.30
−15 °C	0.2637	0.2581	2.12	0.2720	0.2725	0.18	0.2967	0.3012	1.51	0.4388	0.4303	1.93
−10 °C	0.2637	0.2581	2.12	0.3686	0.3586	2.71	0.3995	0.4016	0.53	0.5068	0.5163	1.87
−5 °C	0.2637	0.2581	2.12	0.4928	0.4877	1.03	0.5256	0.5307	0.97	0.5935	0.5881	0.91
0 °C	0.2637	0.2581	2.12	0.6531	0.6598	1.02	0.6805	0.6885	1.17	0.7044	0.7028	0.23
5 °C	0.2637	0.2581	2.12	0.8613	0.8463	1.74	0.8722	0.9036	3.6	0.8477	0.8463	0.16

T_{Cond,CO_2}	$\dot{E}_{D,Comp,NH_3}$			$\dot{E}_{D,EX,NH_3}$			$\dot{E}_{D,Cond,NH_3}$		
	R	M	D	R	M	D	R	M	D
25 °C	2.5382	2.5245	0.54	0.5167	0.5163	0.08	3.0214	3.0123	0.30
−20 °C	1.6390	1.6352	0.23	0.4498	0.4446	1.16	2.0262	2.0225	0.18
−15 °C	1.1200	1.1188	0.11	0.3890	0.3872	0.46	1.5482	1.5491	0.06
−10 °C	0.7925	0.7889	0.45	0.3338	0.3299	1.17	1.2827	1.2909	0.64
−5 °C	0.5740	0.5737	0.05	0.2840	0.2868	0.88	1.1234	1.1332	0.87
0 °C	0.4225	0.4303	1.84	0.2390	0.2438	2.00	1.0255	1.0327	0.70
5 °C	0.3143	0.3155	0.38	0.1985	0.2008	1.16	0.9679	0.9754	0.77

As shown in Fig. 4 and Table 3, the graphs and the achieved values are in accordance, the fact which verifies the sufficient accuracy of the developed model. It is noteworthy to mention that in Table 3, D can be calculated by means of the following formula:

$$D = \frac{R - M}{R} \times 100 \tag{36}$$

5.2. Optimization results

Through the optimization procedure, 4 main design parameters have been taken into account. Table 2 demonstrates the chosen design parameter along with their corresponding range of variations. The tuning parameters which have been chosen for the genetic algorithm optimization procedure are presented in Table 4.

Fig. 5 demonstrates the Pareto optimal solutions achieved from multi-objective optimization of the refrigeration system, in which the mentioned conflict between the considered objectives is clearly demonstrated. As observed in this figure, increasing the exergetic efficiency of the system from 38.41% to 47.74% which is 24% of its initial value, leads to a rise in the total cost rate from 0.0064 US $ s^{-1} to 0.0169 US$ s^{-1} that means a dramatic 164% increase with respect to its initial value.

As shown in Fig. 5, taking into account just the maximization of the exergetic efficiency as the only desired aim results in the selection of point A with the corresponding exergetic efficiency of 47.74% as the optimum point although operating at this point leads to the highest total cost rate (0.0169 US$ s^{-1}). In contrast, the design point B is the most economical point (leading to total cost rate of 0.00764 US$ s^{-1}) that would be chosen, if the total cost rate of the system is considered as the only objective.

In multi-objective optimization problems, all obtained points from the Pareto front are non-dominated and can be chosen as the optimal design point of the plant. However, due to the practical reasons only one optimal solution should be finally selected [22]. Several methods can be employed in the decision-making process in order to select the final optimum design point from the Pareto front obtained through the multi-objective optimization procedure. In most of the multi-objective optimization problems the dimensions of the objectives are different (as in the present work, the total cost rate is expressed in terms of US dollar per unit of time while the exergetic efficiency has no dimension). Hence, before applying the decision making method, the values of objective

Table 4
The tuning parameters in the optimization program.

Tuning parameters	Value
Population size	300
Maximum number of generation	200
Minimum function tolerance	10^{-5}
Probability of crossover	90%
Probability of mutation	1%
Number of crossover point	2
Selection process	Tournament
Tournament size	2

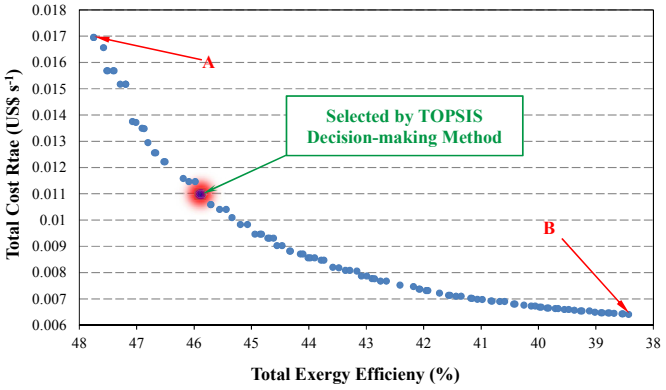

Fig. 5. Pareto optimal frontier from multi-objective optimization of CO_2/NH_3 Cascade refrigeration system.

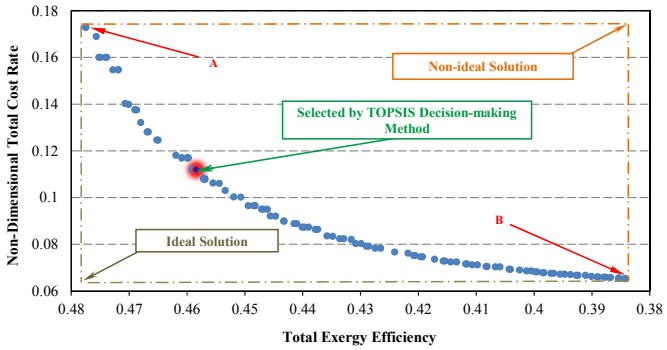

Fig. 6. The set of non-dimensional Pareto optimum solutions using TOPSIS decision-making method to specify the final optimal design point of CO_2/NH_3 Cascade refrigeration system.

functions should be first non-dimensionalized. The Euclidian technique [26] is utilized in the present study to perform the non-dimensionalization procedure. As demonstrated in Fig. 6, after applying the mentioned method, the Pareto optimal solutions are converted into a non-dimensional format.

Once the non-dimensionalization of the objectives is performed, the final optimum design point can be selected using a decision making method. A common decision making method which has been utilized for similar optimization studies in the recent years [22,26–28] is the TOPSIS (Technique for Order Preference by Similarity to an Ideal Solution) decision making method. This method has been shown to be a robust tool for accomplishing decision making procedures after system optimization [27]. In TOPSIS decision making method, which is also employed in the present study, ideal and non-ideal points should be first obtained. The ideal point is the point at which optimum value of each single objective is achieved regardless of satisfaction of other objectives. While, the non-ideal point is defined as the point at which the worst value for each objective is obtained. In fact, the fundamental principle of this approach is that the chosen final optimal point must be in the shortest possible distance from the ideal point and the furthest distance from the non-ideal one [29]. Therefore, both the distance from the ideal point (d^+), and non-ideal point (d^-) are evaluated for all of achieved solution points and the solution with maximum value of the closeness coefficient ($d^-/d^- + d^+$) is selected as the final optimal point, which has been specified in Fig. 5. According to this figure, operating at this point results in exergetic efficiency and total cost rate of 45.89% and 0.01099 US$ s^{-1} respectively.

Table 5 demonstrates the corresponding values of optimal design parameters determined by multi-objective optimization method.

The thermodynamic properties of the critical points of the system while operating at the optimal point obtained from aforementioned optimization approached have been reported in Table 6. Furthermore, the performance-related results of the cascade refrigeration system at the same operating design point are listed in Table 7. In order to take into consideration the change in electricity unit cost, the sensitivity of the Pareto front with the variation in the unit cost of electricity is also investigated and illustrated in Fig. 7. This figure shows that by increasing the unit cost of electricity, the Pareto optimal solutions expectedly move upward (higher total cost) and leftward (higher exergetic efficiency) simultaneously.

Table 5
The optimum values of system design parameters obtained from multi-objective optimization of the system.

Design parameter	Optimal value
T_E (°C)	−48.68
T_{MC} (°C)	−7.06
ΔT_{CAS} (°C)	2.0
T_C (°C)	40.1

Table 6
The thermodynamic properties of the cycle at the final optimum design point derived from TOPSIS decision-making method.

	Temperature (°C)	Pressure (kPa)	Enthalpy (kJ kg^{-1})	Entropy (kJ kg^{-1} K^{-1})
Point 1	−48.68	715.3562	433.0374	2.0954
Point 2	53.21	2862.1	506.9647	2.1323
Point 3	−7.06	2862.1	182.8119	0.9387
Point 4	−48.68	715.3562	182.8119	0.9799
Point 5	−9.1	255.31	1594.8	6.2179
Point 6	135.92	1553.3	1900.8	6.3779
Point 7	40.1	1553.3	533.5442	2.1154
Point 8	−9.1	299.6886	533.5442	2.1966

Finally, Fig. 8 demonstrates the variation in the exergy destruction of different components of the refrigeration system for three different cooling loads of the system while operating at the achieved optimal point. According to this figure, the highest amount of exergy destruction rate takes place in the condenser (3.557 kW, 5.981 kW and 8.285 kW for 30 kW, 50 kW and 70 kW cooling loads respectively). The HTC compressor, LTC expansion valve, LTC compressor, cascade heat exchanger, HTC expansion valve and the evaporator lead to the next highest amounts of exergy destruction rates. Expectedly, increasing the cooling load results in increasing the exergy destruction rates of all components.

6. Conclusion

In the present work, a CO_2/NH_3 cascade refrigeration system was modeled and analyzed from energetic, exergetic, economic, and environmental viewpoints. The developed model was validated using the result of a previous study and employing genetic algorithm technique, the multi-objective optimization of the system was performed to obtain the optimum design parameters of the system. A penalty cost for carbon dioxide production was also considered to take into account the environmental aspects. The exergetic efficiency and the total cost rate (including capital and maintenance costs, operational cost and the penalty cost due to CO_2 emission) were considered as the objective functions in system optimization procedure. Applying the mentioned optimization approach, a set of optimal solutions (called Pareto front) each of which is a tradeoff between the considered objectives was achieved; where the first objective is a thermodynamic indicator and

Table 7
Cascade refrigeration system performance-related results at final optimum design point derived from TOPSIS decision-making method.

Parameter	Value
LTC compressor isentropic efficiency	0.8400
HTC compressor isentropic efficiency	0.7927
CO_2 mass flow rate (kg s^{-1})	0.1998
NH_3 mass flow rate (kg s^{-1})	0.0610
LTC compressor work (kW)	14.7721
HTC compressor work (kW)	18.6755
Overall COP	1.4949
Total exergetic efficiency (%)	45.89
Annual operational cost (US$ $year^{-1}$)	14,048
Annual CO_2 production (Kg $year^{-1}$)	226.6411
Annual CO_2 penalty cost (US$ $year^{-1}$)	20,398
Annual total cost (US$ $year^{-1}$)	277,070

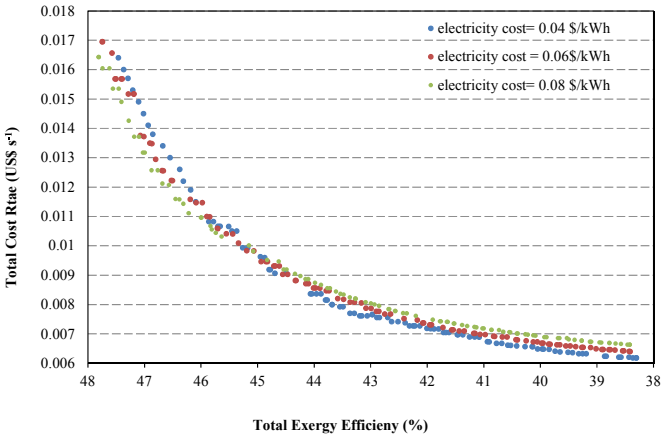

Fig. 7. Sensitivity of Pareto optimal solutions to the electricity unit cost.

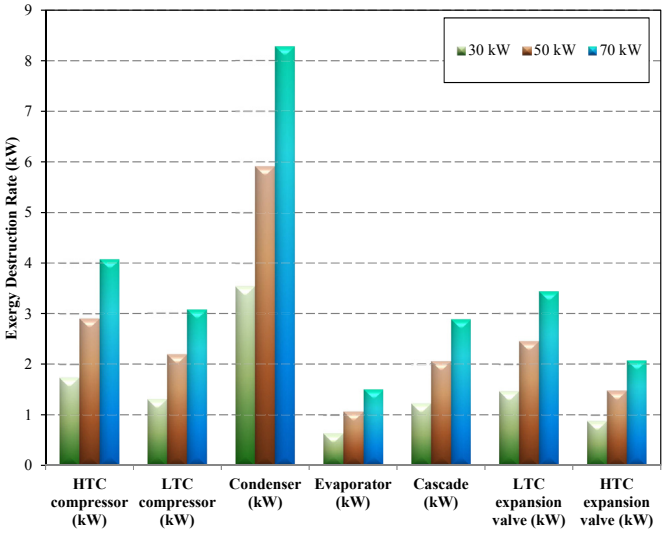

Fig. 8. The exergy destruction values in different components of cascade refrigeration system for three different cooling loads.

the second one is the sum of economic and environmental (emission cost) indicators. The values of achieved solutions were non-dimensionalized in the next step and a final design point was lastly chosen using TOPSIS decision-making technique.

Results of the optimization showed that considering a cooling capacity of 50 kW, the chosen design leads to exergetic efficiency of 45.89% while it results in the total cost rate of 0.01099 US$ s^{-1}, which leads to the total annual cost of 277,070 US$. A sensitivity analysis was performed to investigate the effect of variation of electricity unit cost on achieved Pareto front. The effect of changing the cooling capacity on the exergy destruction through the system while operating at obtained optimum design was also studied.

References

[1] J. Alberto Dopazo, J. Fernández-Seara, J. Sieres, F.J. Uhía, Theoretical analysis of a CO_2–NH_3 cascade refrigeration system for cooling applications at low temperatures, Appl. Therm. Eng. 29 (2009) 1577–1583.

[2] O. Rezayan, A. Behbahaninia, Thermoeconomic optimization and exergy analysis of CO_2/NH_3 cascade refrigeration systems, Energy 36 (2011) 888–895.

[3] T.-S. Lee, C.-H. Liu, T.-W. Chen, Thermodynamic analysis of optimal condensing temperature of cascade-condenser in CO_2/NH_3 cascade refrigeration systems, Int. J. Refrig. 29 (2006) 1100–1108.

[4] A. Pearson, Carbon dioxide—new uses for an old refrigerant, Int. J. Refrig. 28 (2005) 1140–1148.

[5] W. Bingming, W. Huagen, L. Jianfeng, X. Ziwen, Experimental investigation on the performance of NH_3/CO_2 cascade refrigeration system with twin-screw compressor, Int. J. Refrig. 32 (2009) 1358–1365.

[6] H.M. Getu, P.K. Bansal, Thermodynamic analysis of an R744–R717 cascade refrigeration system, Int. J. Refrig. 31 (2008) 45–54.

[7] A. Messineo, R744–R717 Cascade refrigeration system: performance evaluation compared with a HFC two-stage system, Energy Proc. 14 (2012) 56–65.

[8] S. Sanaye, A. Shirazi, Thermo-economic optimization of an ice thermal energy storage system for air-conditioning applications, Energy Build. 60 (2013) 100–109.

[9] R.S. Mitishita, E.M. Barreira, C.O.R. Negrão, C.J.L. Hermes, Thermoeconomic design and optimization of frost-free refrigerators, Appl. Therm. Eng. 50 (2013) 1376–1385.

[10] H. Najafi, B. Najafi, Multi-objective optimization of a plate and frame heat exchanger via genetic algorithm, Heat. Mass Transf./Waerme- Stoffuebertrag. 46 (2010) 639–647.

[11] H. Najafi, B. Najafi, P. Hoseinpoori, Energy and cost optimization of a plate and fin heat exchanger using genetic algorithm, Appl. Therm. Eng. 31 (2011) 1839–1847.

[12] B. Najafi, H. Najafi, M.D. Idalik, Computational fluid dynamics investigation and multi-objective optimization of an engine air-cooling system using a genetic algorithm, Proc. Inst. Mech. Eng., Part C: J. Mech. Eng. Sci. 225 (2011) 1389–1398.

[13] T. Selleri, B. Najafi, F. Rinaldi, G. Colombo, Mathematical modeling and multi-objective optimization of a mini-channel heat exchanger via genetic algorithm, J. Therm. Sci. Eng. Appl. 5 (2013).

[14] A.K. Gholap, J.A. Khan, Design and multi-objective optimization of heat exchangers for refrigerators, Appl. Energy 84 (2007) 1226–1239.

[15] B.H. Gebreslassie, E.A. Groll, S.V. Garimella, Multi-objective optimization of sustainable single-effect water/lithium bromide absorption cycle, Renew. Energy 46 (2012) 100–110.

[16] S. Sanaye, A. Shirazi, Four E analysis and multi-objective optimization of an ice thermal energy storage for air-conditioning applications, Int. J. Refrig. 36 (2013) 828–841.

[17] M. Navidbakhsh, A. Shirazi, S. Sanaye, Four e analysis and multi-objective optimization of an ice storage system incorporating PCM as the partial cold storage for air-conditioning applications, Appl. Therm. Eng. 58 (2013) 30–41.

[18] E. Lemmon, M. McLinden, M. Huber, NIST Fluid Thermodynamic and Transport Properties-REFPROP, Version 7.0 User's Guide, 2004.

[19] T.J. Kotas, Exergy method of thermal and chemical plant analysis, Chem. Eng. Res. Des. 64 (1995).

[20] A. Bejan, G. Tsatsaronis, M. Moran, Thermal Design and Optimization, John Wiley and Sons, New York, 1996.

[21] J. Wang, Z. Zhai, Y. Jing, C. Zhang, Particle swarm optimization for redundant building cooling heating and power system, Appl. Energy 87 (2010) 3668–3679.

[22] A. Shirazi, M. Aminyavari, B. Najafi, F. Rinaldi, M. Razaghi, Thermal–economic–environmental analysis and multi-objective optimization of an internal-reforming solid oxide fuel cell–gas turbine hybrid system, Int. J. Hydrogen Energy 37 (2012) 19111–19124.

[23] A. Konak, D.W. Coit, A.E. Smith, Multi-objective optimization using genetic algorithms: a tutorial, Reliab. Eng. Syst. Saf. 91 (2006) 992–1007.

[24] IPCC, Available from: http://www.ecocostsvalue.com/httpdocs/content/html/2-emissions.html, 2007.

[25] Iranian Central Bank, 2011, URL: http://www.cbi.ir (accessed December 2012).

[26] H. Sayyaadi, R. Mehrabipour, Efficiency enhancement of a gas turbine cycle using an optimized tubular recuperative heat exchanger, Energy 38 (2012) 362–375.

[27] M.H. Ahmadi, H. Sayyaadi, A.H. Mohammadi, M.A. Barranco-Jimenez, Thermo-economic multi-objective optimization of solar dish-Stirling engine by implementing evolutionary algorithm, Energy Convers. Manag. 73 (2013) 370–380.

[28] H.S. Gholamhossein Abdollahi, Application of the multi-objective optimization and risk analysis for the sizing of a residential small-scale CCHP system, Energy Build. 60 (2013) 330–344.

[29] Z. Yue, A method for group decision-making based on determining weights of decision makers using TOPSIS, Appl. Math. Model. 35 (2011) 1926–1936.